JOURNAL OF VIROLOGY, Oct. 2001, p. 9470–9482 Vol. 75, No. 19
0022-538X/01/$04.00+0 DOI: 10.1128/JVI.75.19.9470–9482.2001

A Cellular J-Domain Protein Modulates Polyprotein Processing and Cytopathogenicity of a Pestivirus

G. RINCK,[1]† C. BIRGHAN,[1] T. HARADA,[1]‡ G. MEYERS,[2] H.-J. THIEL,[1] AND N. TAUTZ[1]*

Institut für Virologie (FB Veterinärmedizin), Justus-Liebig-Universität Giessen, D-35392 Giessen,[1] and Federal Research Center for Virus Diseases of Animals, D-72076 Tübingen,[2] Germany

Received 5 April 2001/Accepted 21 June 2001

Pestiviruses are positive-strand RNA viruses closely related to human hepatitis C virus. Gene expression of these viruses occurs via translation of a polyprotein, which is further processed by cellular and viral proteases. Here we report the formation of a stable complex between an as-yet-undescribed cellular J-domain protein, a member of the DnaJ-chaperone family, and pestiviral nonstructural protein NS2. Accordingly, we termed the cellular protein Jiv, for J-domain protein interacting with viral protein. Jiv has the potential to induce in *trans* one specific processing step in the viral polyprotein, namely, cleavage of NS2-3. Efficient generation of its cleavage product NS3 has previously been shown to be obligatory for the cytopathogenicity of the pestiviruses. Regulated expression of Jiv in cells infected with noncytopathogenic bovine viral diarrhea virus disclosed a direct correlation between the intracellular level of Jiv, the extent of NS2-3 cleavage, and pestiviral cytopathogenicity.

Bovine viral diarrhea virus (BVDV) is a member of the genus *Pestivirus* that is grouped together with the genera *Flavivirus* and *Hepacivirus* (hepatitis C viruses) in the family *Flaviviridae* (43). Pestiviruses represent a widely used model system for the human pathogen hepatitis C virus (HCV). Moreover, they are important pathogens of livestock worldwide. The single-stranded RNA genome of BVDV has positive (messenger sense) polarity, is generally 12.3 kb long, and comprises a single long open reading frame (ORF) (3, 29). The encoded polyprotein can be dissected into the N-terminal third encompassing mainly structural components of the virion and the C-terminal part representing the nonstructural (NS) proteins, which are supposed to be part of the viral RNA replication machinery. The first protein of the ORF, N^{pro}, is an autoprotease (35, 49), which releases itself from the remainder of the polyprotein and thereby generates the N terminus of the core protein (C). The latter protein and the envelope glycoproteins E^{rns} (i.e., for RNase secreted) (33), E1 and E2, represent, together with the viral RNA, the major components of the virion (44). Cellular enzymes mediate almost all cleavages in the region of the structural proteins as well as the release of the hydrophobic protein p7. In contrast, the generation of the C terminus of NS protein NS3, as well as all downstream cleavages in the NS region of the polyprotein, are catalyzed by a serine protease located in NS2-3/NS3 (see below); this protease is assisted by its cofactor NS4A (40, 50, 51). NS5A is a phosphorylated protein of unknown function (27). NS5B represents the viral RNA-dependent RNA polymerase (36, 52).

One remarkable feature of BVDV is the occurrence of noncytopathogenic (noncp) and cytopathogenic (cp) virus strains (16). While the noncp viruses replicate without causing obvious morphologic changes in cell culture, infection with cp virus strains induces apoptosis, which can be observed as a cytopathic effect (CPE). At the molecular level the hallmark of cp BVDV-infected cells is the expression of NS3; in contrast, in cells infected with noncp BVDV only unprocessed NS2-3 is detectable. Molecular analyses of cp pestivirus strains revealed various strategies for the generation of NS3 (see below; reviewed in reference 23). In many cases NS3 is produced by NS2-3 cleavage. Based on infectious pestiviral cDNA genomes, it was demonstrated that the efficient generation of NS3 is essential for the cytopathogenicity of the virus (14, 17, 20, 39). cp BVDV strains evolve from noncp ancestor viruses, often by RNA recombination, in the course of a lethal disease of cattle (23). In several cp BVDV genomes, insertions of fragments of cellular mRNAs were detected, most frequently insertions of cellular ubiquitin-coding sequences (19). In the viral polyprotein, these insertions always were localized right upstream of NS3; the inserted ubiquitin was shown to provide a cleavage site for cellular ubiquitin-specific proteases and thus leads to an efficient release of NS3 (42).

In the RNA genome of several cp BVDV strains a cell-derived insert, previously termed cINS, was identified (18, 30, 47). Partial cDNA cloning of the corresponding cellular mRNA revealed an identity of 99% at the nucleotide level (18). On the basis of the fragmentary sequence data, no conclusive hypothesis for a function of the derived peptide was published. According to the results obtained by the present study (see below), we now term the corresponding gene and mRNA jiv and the derived protein Jiv (for J-domain protein interacting with viral protein). In contrast to the insertions of ubiquitin-coding sequences described above, the Jiv insertion is located within the NS2 protein of BVDV, in strain NADL 53 amino acids upstream of the NS2-3 cleavage site (17). In the context of an infectious cDNA clone of BVDV NADL, a jiv insertion with a length of 90 codons was shown to be essential

* Corresponding author. Mailing address: Institut für Virologie (FB Veterinärmedizin), Justus-Liebig-Universität Giessen, Frankfurter Strasse 107, D-35392 Giessen, Germany. Phone: 49 (641) 99-38375. Fax: 49 (641) 99-38359. E-mail: Norbert.Tautz@vetmed.uni-giessen.de.

† Present address: Virco UK, Ltd., Cambridge, United Kingdom.

‡ Present address: Chiron Corp., I-53100 Siena, Italy.

for NS2-3 cleavage and thereby for the cp phenotype of the virus (17). However, the mechanism of cleavage and especially the function of the cellular sequence in this process remained obscure.

Here we report that complete cellular Jiv and Jiv90, the latter corresponding to the fragment of Jiv identified as an insertion in BVDV strain NADL, undergo a stable interaction with viral NS2 and stimulate cleavage of noncp BVDV-derived NS2-3 in *trans*. Our data provide evidence that the intracellular level of Jiv modulates pestiviral polyprotein processing and thereby determines the viral phenotype.

MATERIALS AND METHODS

Cells and viruses. Madin-Darby bovine kidney (MDBK) cells were obtained from the American Type Culture Collection (Rockville, Md.). BHK-21 cells were kindly provided by J. Cox (Federal Research Center for Virus Diseases of Animals, Tübingen, Germany). Cells were grown in Dulbecco modified Eagle medium (DMEM) supplemented with 10% fetal calf serum (FCS). Cells were maintained at 37°C and 5% CO_2. The recombinant vaccinia virus expressing the T7 RNA polymerase [modified virus Ankara (MVA-T7pol)] (37) was generously provided by G. Sutter (Institut für Molekulare Virologie, GSF-Forschungszentrum für Umwelt und Gesundheit GmbH, Oberschleissheim, Germany). The noncp BVDV strain NCP7 was described previously (5).

BVDV infection. After removal of the medium, the cells were washed with DMEM lacking FCS and incubated in the latter medium with BVDV strain NCP7 at a multiplicity of infection (MOI) of between 0.01 and 0.5. After 1 h the supernatant was replaced by DMEM including FCS.

Transient expression with the T7 vaccinia virus system. BHK-21 cells (5×10^5, 3.5-cm dish) were infected with MVA-T7pol at an MOI of 1 in medium lacking FCS. After 1 h at 37°C, the cells were washed with phosphate-buffered saline (PBS) and transfected with 1.5 μg of each plasmid DNA by the use of Superfect (Qiagen, Hilden, Germany). For Western blot analysis the transfected cell cultures were harvested about 6 h posttransfection (p.t.).

Radioactive labeling of cells. At 2 h p.t., cells were washed with PBS and incubated for 60 min with 1 ml of DMEM without cysteine and methionine at 37°C. After the addition of 500 μl of labeling medium containing 70 μCi of [^{35}S]-labeled methionine and cysteine ([^{35}S]-ProMix; Amersham, Freiburg, Germany), protein expression was allowed to proceed for an additional 4 h at 37°C. After a rinse with PBS, cells were lysed in radioimmunoprecipitation assay (RIPA) buffer (50 mM Tris-HCl [pH 8.0], 150 mM NaCl, 1% [vol/vol] NP-40, 1% [wt/vol] deoxycholate, 0.1% [wt/vol] sodium dodecyl sulfate [SDS], 0.5 mM PefablocSC [Merck, Darmstadt, Germany]) and subsequently frozen at −70°C.

RIPA. Cell lysates were cleared by centrifugation at 12,000 × *g* for 20 min at 4°C prior to the addition of the specific antibody or antiserum. After incubation for 1 h at 4°C, the lysates were mixed with 0.5 volume of 10% (vol/vol) protein A-Sepharose (Sigma Chemical Co., St. Louis, Mo.), which was previously cross-linked with rabbit immunoglobulin (10a) directed against the Fc fragment of mouse immunoglobulin G (IgG; Cappel/Organon Teknika Co., West Chester, Pa.). After 1 h at 4°C, the precipitates were collected by centrifugation at 3,000 × *g* for 5 min and washed three times with RIPA buffer. Precipitates were resuspended in SDS-sample buffer (2% [wt/vol] SDS, 10% [vol/vol] glycerol, 6 M urea, 5% [vol/vol] β-mercaptoethanol, 0.01% [wt/vol] bromphenol blue) and boiled for 5 min prior to analysis by SDS-polyacrylamide gel electrophoresis (PAGE). Gels were fixed and processed for fluorography with Enlightning solution (NEN Life Science, Zavantem, Belgium).

SDS-PAGE and immunoblotting. Proteins were separated in 6 to 12% polyacrylamide Tricine gels (32). After SDS-PAGE, the proteins were transferred onto nitrocellulose membrane (Optitran BA-S83 reinforced NC; Schleicher & Schuell, Düren, Germany); the membrane was blocked with 3% (wt/vol) dried skimmed milk in TPBS (0.05% [vol/vol] Tween 20 in PBS). For the detection of antigen, peroxidase-coupled species-specific secondary antibodies and Renaissance Western blot Chemiluminescence Reagent Plus (NEN/Life Sciences, Boston, Mass.) were applied.

Antibodies and antisera. The anti-Flag M2 monoclonal antibody (MAb) was purchased from Sigma and was used according to the recommendations of the supplier. The anti-GST MAb (hybridoma supernatant) was kindly provided by J. Richt (Institut für Virologie, Justus-Liebig-Universität, Giessen, Germany). For the detection of NS3, mouse MAb 8.12.7 (4) was used. Generation of the anti-Jiv serum (previously termed anti-cINS serum) in rabbits has been described elsewhere (1). Peroxidase- or cyanogen 3 (Cy3)-coupled secondary antibodies directed against mouse or rabbit immunoglobulin were purchased from Dianova (Hamburg, Germany).

Phage libraries. Clone cIK9 was isolated from a commercial Lambda ZAP II based cDNA library of MDBK cells (Stratagene, La Jolla, Calif.). The randomly primed clone cIK9-4 was identified in a self-established cDNA library primed on mRNA from MDBK cells. For cloning and packaging, Lambda ZAP II vector and Gigapack III Gold packaging extracts (Stratagene) were used. The general protocol used to establish the cDNA library was published previously (21). Initial screening was carried out with a 270-bp fragment of jiv, which was identified in the genome of BVDV strain NADL (18). Clones cIK9 and cIK9-4 encompass nucleotides (nt) 963 to 3159 and nt 332 to 2963 of the obtained jiv-cDNA sequence, respectively.

RNA preparation, gel electrophoresis, and Northern blot. Total RNA from MDBK cells was prepared by using RNeasy total RNA kit (Qiagen) or by centrifugation through a CsCl cushion as previously described (21). For isolation of poly(A)$^+$ RNA from MDBK cells, the PolyATract System II (Promega, Mannheim, Germany) was used. For the Northern blot in Fig. 1A, 5 μg of glyoxylated poly(A)$^+$ RNA was separated in a formaldehyde-containing agarose gel and hybridized to a [α-^{32}P]dCTP-labeled cDNA probe encompassing nt 963 to 3159 of the jiv-cDNA. The protocols for nick translation, gel electrophoresis, and Northern blotting were described previously (41).

PCR. PCR and reverse transcription-PCR (RT-PCR) were carried out as described previously (22, 40) using a Genius thermocycler (Techne/Thermodux, Wertheim, Germany) and total RNA from MDBK cells as a template. The primers used for the RT-PCR amplification of different jiv-mRNA fragments (Fig. 1B) were as follows: SmaA/KpnB (fragment 1, nt 152 to 554), KpnA/NcoB (fragment 2, nt 493 to 1524), NcoA/SspB (fragment 3, nt 1457 to 2405), and SspA/End (fragment 4, nt 2338 to 3028). The 3′-terminal part of the jiv-mRNA was analyzed by RT using primers NcoA and T_{15} (oligo-dT_{15}), followed by a standard PCR using primers T_{15} and cins+. For the analysis of the 5′-terminal part of the jiv-mRNA, an RT followed by a ligation anchored-PCR was accomplished. By using the thermostable reverse transcriptase CombiScript (Pan Biotech, Aidenbach, Germany), 1.5 μg of mRNA was transcribed at 70°C for 20 min in the supplied reaction buffer supplemented by 1 mM $MnCl_2$, 250 μM concentrations of deoxynucleoside triphosphates, 1 U of RNaseOUT (Life Technologies, Karlsruhe, Germany)/μl, and 3 μM antisense primer KpnBlang. After the RNA was degraded by alkaline hydrolysis, one-third of the cDNA was subjected to ligation with 10 pmol of primer Ifflig, which was phosphorylated at its 5′ end and 3′-terminally blocked by an amino group; the ligation reaction was carried out by T4 RNA ligase (MBI Fermentas, Vilnius, Lithuania) for 24 h at room temperature in the supplied reaction buffer supplemented with 20 μM ATP, 10 μg of bovine serum albumin/ml, and 20% (wt/vol) polyethylene glycol. The ligation product served as a template for a nested PCR. Primers M13rev (complementary to the 3′ half of primer Ifflig) and KpnB were used for the primary PCR; for the nested PCR primers M13 (complementary to the 5′ half of primer Ifflig) and SmaB were applied. The PCR product was cloned by the use of pGEM-T Vector System I (Promega), and the sequence of the cDNA inserts was determined. The longest sequence identified downstream of primer Ifflig was represented by several clones in two independent experiments. Therefore, we assume that the obtained cDNA sequence (see Fig. 1C) represents the entire jiv-mRNA. Fragment 0 (Fig. 1B) thus encompassed bp 1 to 203 of the jiv-cDNA.

Construction of expression plasmids. For cloning of PCR-derived jiv-cDNA fragments, the pGEM-T Vector System I (Promega) was used. Subsequently, the jiv-cDNA (nt 1 to 3027) was assembled by standard cloning techniques. A cDNA fragment encompassing the entire Jiv-ORF was ligated into plasmid pTRE (Clontech, Palo Alto, Calif.). The resulting plasmid pTRE/Jiv encompassed nt 188 to 2516 of the jiv-cDNA and encodes the authentic 699 codon ORF of Jiv. Expression from this construct was controlled by the Tet-responsive element combined with a minimal cytomegalovirus promoter (8).

pJiv is based on pBluescript II SK(−) (Stratagene), encompasses nt 183 to 2513 of the jiv-cDNA, and encodes the authentic 699 codon ORF under the control of the T7 RNA polymerase promoter.

In vector pCITE (Novagen, Madison, Wis.), the internal ribosomal entry site (IRES) of encephalomyocarditis virus is located downstream of the T7 promoter to enhance Cap-independent translation in the context of the MVA-T7pol vaccinia virus expression system. pJiv90 is based on pCITE and encodes two PCR-derived amino acids (methionine and glycine), followed by amino acids 533 to 622 of Jiv downstream of the IRES. For the construction of pGST-Jiv and pGST-Jiv90, pCITE-GST (40) was used, which encodes glutathione *S*-transferase (GST) downstream of the IRES. In pGST-Jiv and pGST-Jiv90 the complete 699 codon frame or codons 533 to 622 of the jiv-cDNA are fused in frame to the C terminus of GST, respectively. pC/E2-4A is based on pCITE and encodes amino acids 693 to 2343 of the polyprotein of BVDV strain CP7 (41)

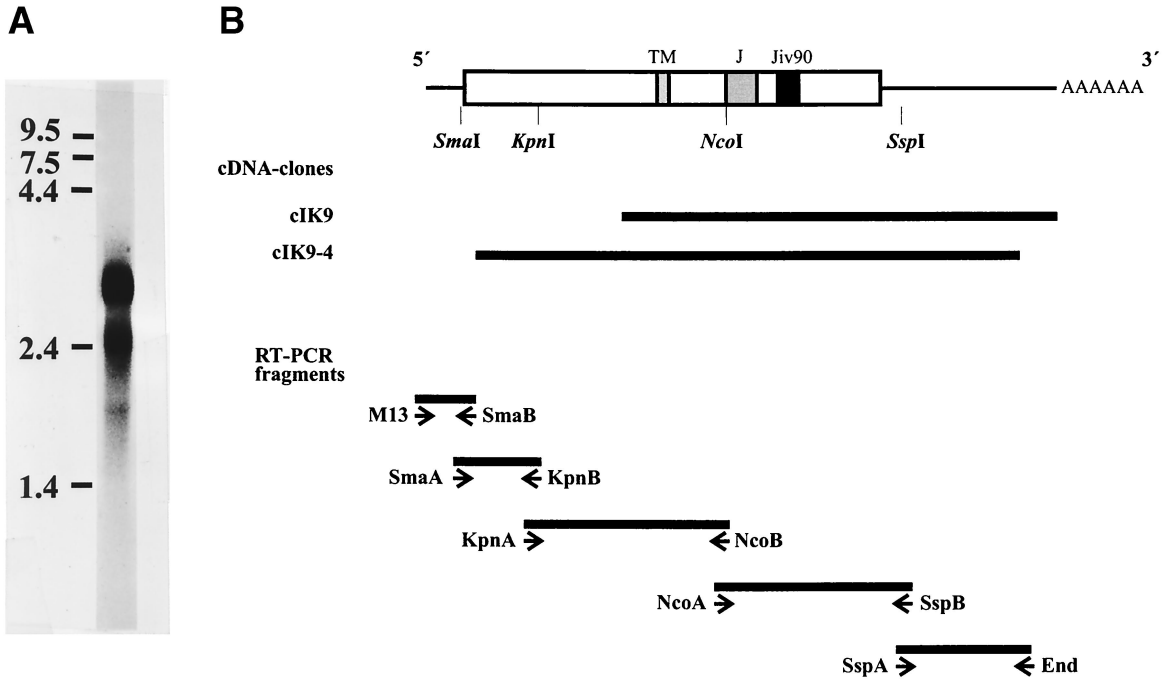

FIG. 1. (A) Northern blot. Poly(A)$^+$ RNA from MDBK cells was separated under denaturing conditions on a 0.8% agarose gel and blotted onto a Duranlon-UV membrane (Stratagene). The blot was hybridized with a jiv-specific probe labeled with [α-^{32}P]dCTP. The numbers at the left side indicate the size of the RNA marker in kilobases. (B) cDNA cloning of the jiv-mRNA. In the upper part of the figure, the bar symbolizes the Jiv protein; different domains are pointed out on top as follows: TM, putative transmembrane region; J, J domain; and Jiv90, Jiv90 domain. The lines at both ends symbolize the noncoding regions of the mRNA. The relative positions of the restriction sites used to establish a cDNA clone encompassing the entire jiv-ORF are indicated. The cDNA library-derived clones cIK9 and cIK9-4 are shown as black bars. In the lower part of the figure, the RT-PCR fragments established to verify and complete the cDNA cloning are depicted as solid bars. The primers used for amplification are symbolized by arrowheads below. Primer M13 was complementary to the 5′ sequence of the oligonucleotide, which was ligated to the first-strand cDNA in order to analyze the 5′ end of the mRNA. (C) Nucleotide and deduced amino acid sequences of the cDNA representing the jiv-mRNA. Domains: putative transmembrane domain (amino acids 327 to 347); J domain (boldface; amino acids 444 to 505); Jiv90 domain (underlined; amino acids 533 to 622) with CXXCXXXH motifs (underlined and boldface). The shorter mRNA ends with nt 2402.

preceded by a foreign signal sequence (10). In the NS2 gene of BVDV CP7, a strain-specific 27-base insertion has been identified; this insertion was shown to be essential for the induction of NS2-3 cleavage (41); the deletion of the corresponding insertion from the NS2 gene in pC/E2-4A led to construct pN/E2-4A, which displays no processing of NS2-3. pFlagNS2 is based on pCITE and encodes downstream of the AUG start codon the Flag-epitope (DYKDDDK), followed by a leucine residue and NS2 of BVDV CP7ins− (amino acids 1137 to 1580) (41).

pcEF$_{\text{Tet-On}}$/NEO. The ORF of the Tet-activator protein rtTA (8) was amplified from pTet-On (Clontech) by PCR and inserted into the *Swa*I site of cdEF321swxneo (9). The resulting plasmid, pcEF$_{\text{Tet-On}}$/NEO, encompasses the neomycin resistance gene and the rtTA ORF under the control of the human elongation factor 1α (EF-1α) promoter.

pEF-Pac. The puromycin *N*-acetyltransferase gene (Pac) was amplified from pSINrep19 (7) and cloned into the *Xba*I site of vector pEF-BOS (24), resulting in plasmid pEF-Pac. In the latter vector the EF-1α promoter maintains Pac expression.

Nucleotide sequencing and sequence analysis. Nucleotide sequencing was described previously (40). Computer analysis of sequence data was performed by use of the program package HUSAR (DKFZ, Heidelberg, Germany), including the University of Wisconsin Genetics Computer Group (GCG) software package (6). Database searches were carried out by the use of FASTA or TFASTX. Genomic sequences were analyzed by GENSCAN. Multiple alignment of amino acid sequences was generated by CLUSTAL. The jiv-cDNA sequence was also analyzed by SMART (EMBL, Heidelberg, Germany) (34) and PSORT (25).

Establishment of MDBK$_{\text{Tet-On}}$/Jiv cell line. To express Jiv in the BVDV host cells (MDBK) in a regulated fashion, the Tet-On expression system was applied (8). To establish the basic cell line MDBK$_{\text{Tet-On}}$, which expresses the activator protein rtTA constitutively, 2 μg of linearized pcEF$_{\text{Tet-On}}$/NEO was electroporated into 3×10^6 MDBK cells at 960 μF and 1,100 V/cm by using a Gene Pulser II (Bio-Rad, Munich, Germany). At 3 days p.t. the culture medium was replaced by a selection medium containing 1 g of G418 (Calbiochem, Frankfurt, Germany)/liter. G418-resistant colonies were isolated and replated twice for purification. Expression of rtTA in each clone was monitored by transfection of pBI-GL (Clontech) according to the manufacturer's instructions. The resulting MDBK$_{\text{Tet-On}}$ cell line was transfected (see above) with 5 μg of pTRE-Jiv and 150 ng of pEF-Pac both linearized with *Hin*dIII. For selection, the cell culture medium was replaced at 3 days p.t. by medium containing 100 mg of G418 and 5 mg of puromycin/liter. Resistant colonies were isolated and replated for purification. The resulting MDBK$_{\text{Tet-On}}$/Jiv cell clones were monitored for inducible expression of Jiv by indirect immunofluorescence with anti-Jiv serum at 36 h after the addition of 10 μM doxycycline (Dox).

Indirect immunofluorescence and confocal laser-scanning microscopy. Cells were seeded on cover slides and, after two washes with PBS, were fixed with 4% (wt/vol) paraformaldehyde in PBS for 25 min at 4°C. Permeabilization was achieved by incubation with 1% (wt/vol) *N*-octyl-β-D-glycopyranoside for 5 min at 4°C. After a wash with PBS, the cells were incubated at 37°C with anti-Jiv serum in a dilution of 1:500 in PBS. Secondary antibodies labeled with Cy3 were used according to the instructions of the manufacturer. For the analysis the confocal laser-scanning microscope TCS-NT was coupled to the microscope DM IRBE (Leica, Wetzlar, Germany) at the following settings: filter settings DTAF (dichlorotriazinyl aminofluorescein)/TRITC (tetramethyl rhodamine isothiocyanate)/Cy5/spec; the bypass filter was BP600/30; the accumulation was set to 4; and the pinhole setting was 1.

Sequences of the oligonucleotide primers. In the following primers, the polarity is indicated by a "+" for sense orientation or a "−" for antisense orientation: SmaA, GGCTGTGACTTAAAATCCTCAG (+); KpnB, GGAAAGGAAAGA AGAGTTCCC (−); KpnA, GTGGACAGGAACTCTCAAGAG (+); NcoB, AAAGGGTTTAGCTCATCCTC (−); NcoA, CCAGCCTGAAGAGGAAGT GGC (+); SspB, TTTGAGCTTAAAATTTTCCC (−); SspA, ACAGCACAG

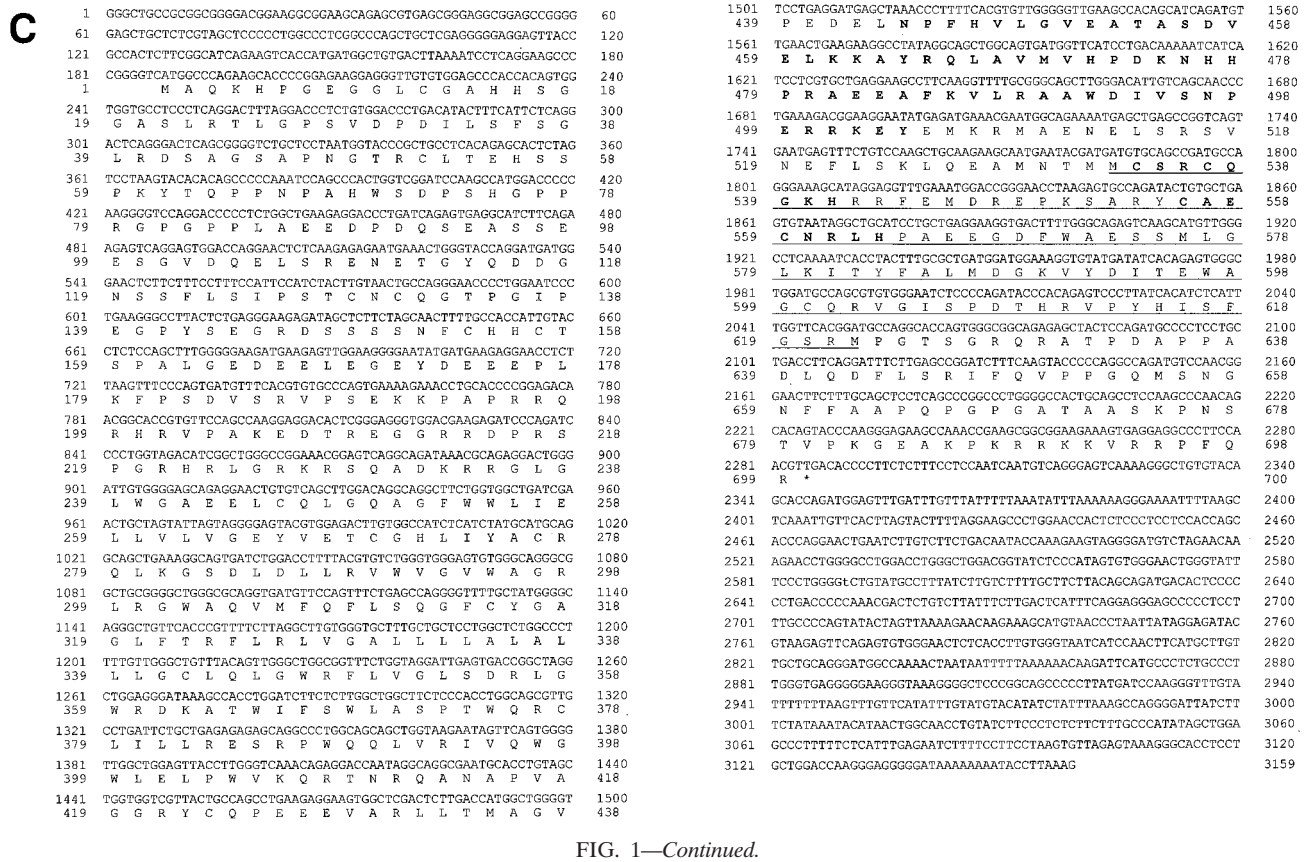

FIG. 1—*Continued.*

ATGGAGTTTG (+); End, TTTACAGGTTGCCCGTTATG (−); cins+, TCG CGAAATGTGCAGCCGATGCCAGGG (+); KpnBlang, AGATGGAATGG AAAGGAAAGAAGAGTTCCC (−); Ifflig, TACTGGCCGTCGTTTTACAT GGTCATAGCTGTTTCC blocked at the 3′ end by an amino group; M13rev, GGAAACGCTATGACCATG (complementary to the 3′ part of primer Ifflig); M13, GTAAAACGACGGCCAGT (complementary to the 5′ part of primer Ifflig); and SmaB, GGTGCTTCTGGGCCATGAC (−).

Sequence accession numbers. Sequence data from this article have been deposited with the EMBL/GenBank data libraries under accession no. AY027881 and AY027882.

RESULTS

cDNA cloning of cellular jiv mRNAs. For cp BVDV strain NADL, an insertion of 90 Jiv-derived amino acids in NS2 has been shown to be required for cleavage of NS2-3 and thereby for generation of NS3, the marker protein of cp BVDVs (17). To gain insight into the function of Jiv in this cleavage event, we decided to first characterize cellular Jiv by cDNA cloning of the corresponding cellular mRNAs.

The starting material for this analysis was the bovine kidney cell line MDBK. In a Northern blot on poly(A)$^+$ RNA of MDBK cells, a jiv-cDNA probe detected two RNA species of ca. 3.2 and 2.6 kb (Fig. 1A). From MDBK cDNA libraries, cDNA clones cIK9 and cIK9-4 were isolated, which encompassed jiv-specific cDNA inserts of 2.2 and 2.7 kb, respectively (Fig. 1B). A comparison of these clones revealed that clone cIK9-4 ends with nt 192 upstream of the poly(A) sequence present in clone cIK9 (Fig. 1B); accordingly, clone cIK9-4 was randomly primed in the 3′ region of the jiv-mRNA. With respect to these clones, a ligation-anchored-PCR analysis identified additional sequences at the 5′ end of the jiv-mRNA (see Materials and Methods). With a total length of 3,159 bases [without a poly(A) tail], the established jiv-cDNA sequence (Fig. 1C) apparently represents the complete 3.2-kb jiv-mRNA species identified in the Northern blot. A series of RT-PCR analyses verified the obtained sequence (Fig. 1B) but gave no indication for the existence of a shorter jiv-mRNA species encompassing internal deletion(s) in the ORF (data not shown). To characterize the shorter jiv-mRNA observed by Northern blotting, we looked for jiv-mRNA species encompassing a truncated 3′ untranslated region (UTR). By using an oligo(T) primer and a jiv-specific forward primer, an additional shorter jiv-specific cDNA fragment was obtained (see Materials and Methods). Compared to clone cIK9, the DNA sequence of the short RT-PCR fragment had a deletion of 757 bases upstream of the poly(A) tail. This finding strongly suggests that the size difference observed between the jiv-mRNA species in the Northern blot is caused by variations in their 3′ UTRs. Taken together, the lengths of the identified cDNA sequences match the data obtained by Northern blotting.

Amino acid motifs in Jiv. A computer-assisted analysis (SMART program [34]) of the deduced amino acid sequence of Jiv indicated the presence of an internal transmembrane region and a so-called J domain (Fig. 1C). J domains in general have a length of ca. 70 amino acids and represent the common characteristic for the otherwise highly heterogeneous DnaJ family of chaperones (reviewed in references 2 and 12). J

domains have been implicated in mediating a specific binding to members of the heat shock protein 70 (Hsp70) family. Downstream of the J domain, two CXXCXXXH motifs reside (Fig. 1C); C or H represents a cysteine or a histidine residue, while X represents any amino acid. In the Zn^{2+}-binding domain of the *Escherichia coli* Hsp DnaJ, the thoroughly investigated founding member of the J-domain family, similar motif pairs were identified (see Discussion) (38).

Database searches identified orthologs of Jiv in different species. While the Jiv orthologs of *Caenorhabditis elegans* and *Arabidopsis thaliana* were identified as hypothetical proteins in protein databases, Jiv of *Drosophila melanogaster*, as well as the human ortholog, was assembled based on a GENSCAN (GCG software package [6]) analysis of genomic DNA sequences. The corresponding sequences are depicted in a multiple alignment (Fig. 2), which reveals a high phylogenetic conservation, especially for the J domain, the two CXXCXXXH motifs, and the Jiv90 peptide, which corresponds to the Jiv fragment identified previously as insertion in NS2 of BVDV strain NADL. In the Jiv90 domain, the C-terminal amino acid represents the only amino acid exchange observed between human and bovine Jivs.

In the bovine jiv-mRNA, the longest ORF starting with an AUG codon has a length of 699 codons and is in frame with the Jiv90 peptide. This ORF begins at the third AUG codon ($AUG_{188–190}$) comprising nucleotides 188 to 190 of the jiv-mRNA; according to the rules of Kozak (13) the respective AUG should allow efficient translation initiation (Fig. 1C). The first AUG codon (bases 147 to 149), which is directly followed by the second AUG triplet, lies in a different reading frame; the respective ORF has a length of five codons and thus terminates upstream of $AUG_{188–190}$. Upstream of the 699-amino-acid ORF, no stop codon was identified in the same frame. We could therefore not definitely exclude the theoretical possibility that the ORF of authentic Jiv starts at an AUG codon in an unidentified upstream part of the jiv-mRNA. Even though this appeared to be highly unlikely (also see above), we tried to verify the authenticity of $AUG_{188–190}$ as an initiation codon of Jiv by comparing the apparent molecular weights of the recombinant Jiv ORF with 699 codons with authentic Jiv from MDBK cells. However, due to the low expression level of Jiv in MDBK cells, we were not able to identify this protein unambiguously with the immunological reagents currently available (data not shown). As an alternative approach, we performed database searches to identify the N termini of Jiv orthologs in other species. Six expressed sequence tag sequences representing the 5′ region of mouse jiv-mRNA were found. The mouse ortholog showed in the N-terminal 84 amino acids an identity of ca. 86% to bovine Jiv (data not shown). In five of these sequences the start AUG was preceded by in-frame stop codons (data not shown). This finding verified that the ORF of mouse Jiv starts with the AUG corresponding to $AUG_{188–190}$ in the bovine jiv-mRNA. According to the amino acid sequence assembled from a GENSCAN analysis of genomic DNA, the human Jiv ortholog showed an amino acid identity of ca. 91% to bovine Jiv and also starts with the corresponding AUG (data not shown). On the basis of these analyses and our experimental data, it is considered highly likely that $AUG_{188–190}$ represents the authentic start codon of the bovine jiv-mRNA.

Stimulation of NS2-3 cleavage in *trans*. Each J-domain protein undergoes different protein-protein interactions. To fulfill this function, J-domain proteins encompass independent protein-binding domains (see Discussion). In the context of our system, these facts implied that Jiv might interact with viral NS2-3 and thereby could induce its cleavage.

To test this hypothesis, we investigated the processing of pestiviral NS2-3 by using the T7-vaccinia virus system. BHK-21 cells were infected with recombinant vaccinia virus MVA-T7pol expressing the RNA polymerase of bacteriophage T7 (37) and subsequently transfected with relevant T7 expression plasmids. For initial experiments, we used plasmids pN/E2-4A, encoding an E2-to-NS4A polyprotein fragment derived from a noncp BVDV strain (CP7ins−) (20, 41), and pJiv, encompassing the complete ORF with 699 amino acids (Fig. 3). In cells transfected with pN/E2-4A, the viral NS2-3 protein with an apparent molecular mass of about 125 kDa could be detected by an NS3-specific MAb (i.e., anti-NS3 MAb) in a Western blot analysis (Fig. 4, lane 2). Upon cotransfection of pJiv and pN/E2-4A, an additional protein with an apparent molecular mass of 80 kDa was detected (Fig. 4, lane 3), which comigrated with NS3 expressed from control plasmid pC/E2-4A (Fig. 4, lane 5). The latter encodes the polyprotein of a cp BVDV strain (CP7) from E2 to NS4A; an efficient release of NS3 from this polypeptide has been demonstrated previously (20, 41). According to these data, Jiv indeed has the capacity to induce in *trans* efficient cleavage of NS2-3.

As already mentioned above, the insertion of 90 Jiv-derived amino acids into NS2 of cp BVDV strain NADL induced NS2-3 cleavage (17). Taking into account our finding that complete Jiv induces NS2-3 cleavage in *trans*, it was reasonable to assume that the Jiv90 peptide corresponding to the Jiv fragment identified in strain NADL might also be able to induce NS2-3 cleavage in *trans*. To test this hypothesis, we coexpressed NS2-3 of noncp BVDV together with Jiv90 by the simultaneous transfection of plasmids pN/E2-4A and pJiv90 (Fig. 3) into cells preinfected with vaccinia virus MVA-T7pol. In a Western blot analysis of the respective cell lysates, the anti-NS3 MAb detected apart from NS2-3 a major amount of NS3. The appearance of NS3 indicated efficient processing of NS2-3 (Fig. 4, lane 4). Thus, both complete Jiv and also the Jiv90 peptide can induce efficient cleavage of NS2-3 in *trans*. The lower extent of NS2-3 cleavage induced by Jiv compared to Jiv90 is most likely caused by differences in the expression level of both proteins due to the use of different vector backbones (see Materials and Methods). This assumption is substantiated by the observation that GST-Jiv and GST-Jiv90 display no obvious differences with respect to the induction of NS2-3 cleavage (see also below).

Interaction between NS2 and Jiv. The fact that complete Jiv, as well as its fragment Jiv90, induces the cleavage of NS2-3 strongly suggested an interaction between these proteins. We therefore attempted to demonstrate binding of Jiv to NS2-3. For this study, we first constructed the T7 expression plasmid pFlag-NS2 encoding the NS2 protein of a noncp BVDV strain (CP7ins−) preceded by an N-terminal Flag-tag (Fig. 3). In addition, pNS3, which encodes the viral polyprotein from NS3 down to a C-terminally truncated NS4B (data not shown), was used. pGST-Jiv and pGST-Jiv90 encode full-length Jiv and Jiv90, respectively, fused in frame to the C terminus of GST.

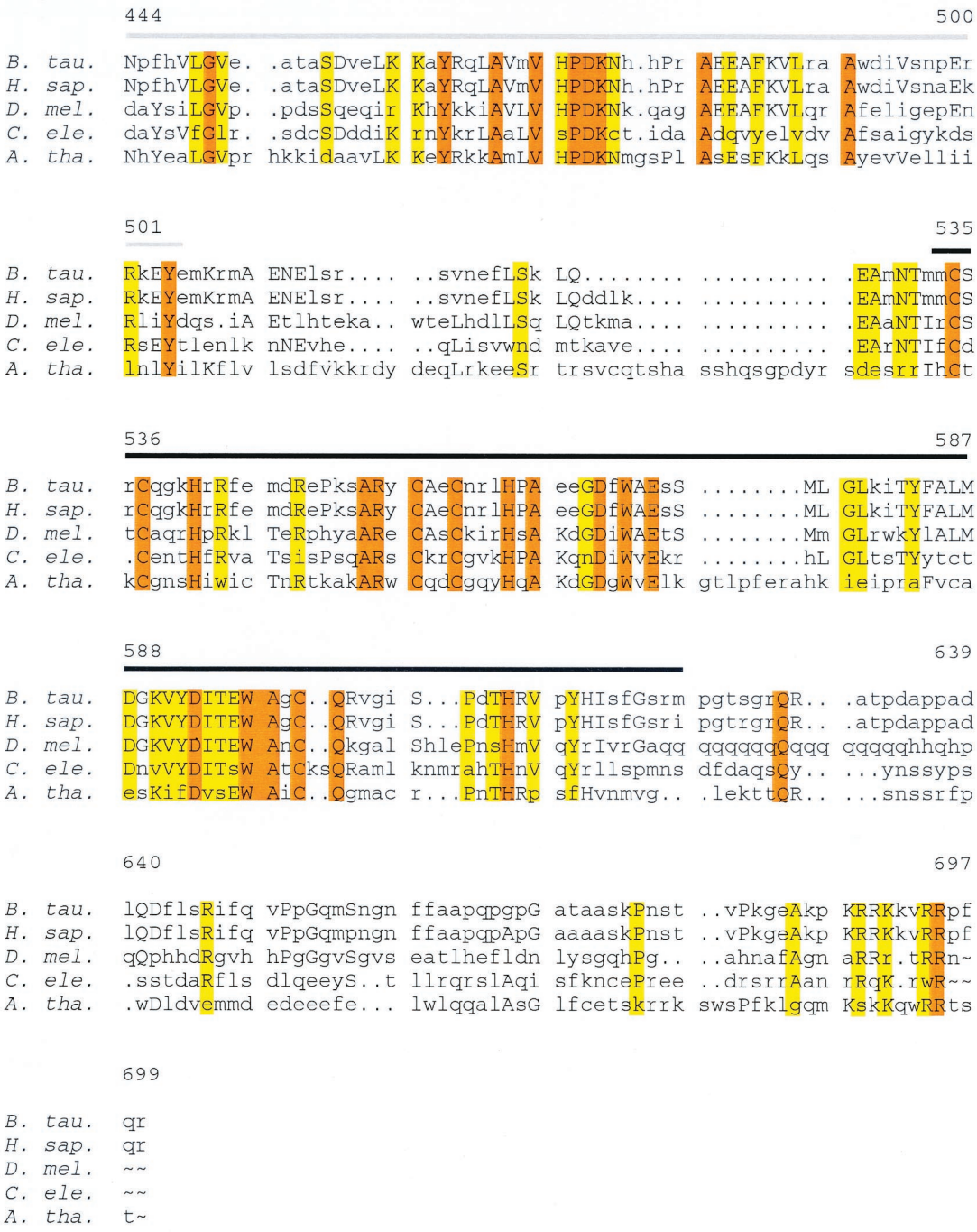

FIG. 2. Multiple alignment of bovine Jiv and Jiv orthologs from other species starting with the J domain. The J domain is marked by a gray line, and the Jiv90 domain is marked by a black line. Coding: capital letters, amino acids conserved between more than two species; yellow, amino acid identical in four of five species; red, conserved amino acid. Abbreviations: *B. tau.*, *Bos taurus* (this study); *H. sap.*, *Homo sapiens* (derived from a GENSCAN analysis of genomic clone AC023055); *D. mel.*, *Drosophila melanogaster* (derived from a GENSCAN analysis of genomic clone AC014875); *C. ele.*, *Caenorhabditis elegans* (hypothetical protein CO4A2.7) (Q09446); *A. tha.*, *Arabidopsis thaliana* (hypothetical protein YUP8H12R.35) (T01052).

These expression plasmids were used for transient-expression studies in BHK-21 cells infected with vaccinia virus MVA-T7pol. The fusion of GST to Jiv or to Jiv90 did not interfere with their ability to induce the cleavage of NS2-3 (Fig. 4, lanes 7 and 8). For the coprecipitation study, metabolic labeling was performed with [^{35}S]methionine and [^{35}S]cysteine. The respective cell lysates were prepared under nondenaturing conditions and subjected to immunoprecipitation applying a Flag-tag- or a GST-specific MAb. After cotransfection of pFlag-NS2 and pGST-Jiv, the anti-Flag MAb, as well as the anti-GST MAb, pulled down polypeptides with molecular masses of 40 and 110 kDa (Fig. 5, lanes 5 and 6). These proteins comigrated with

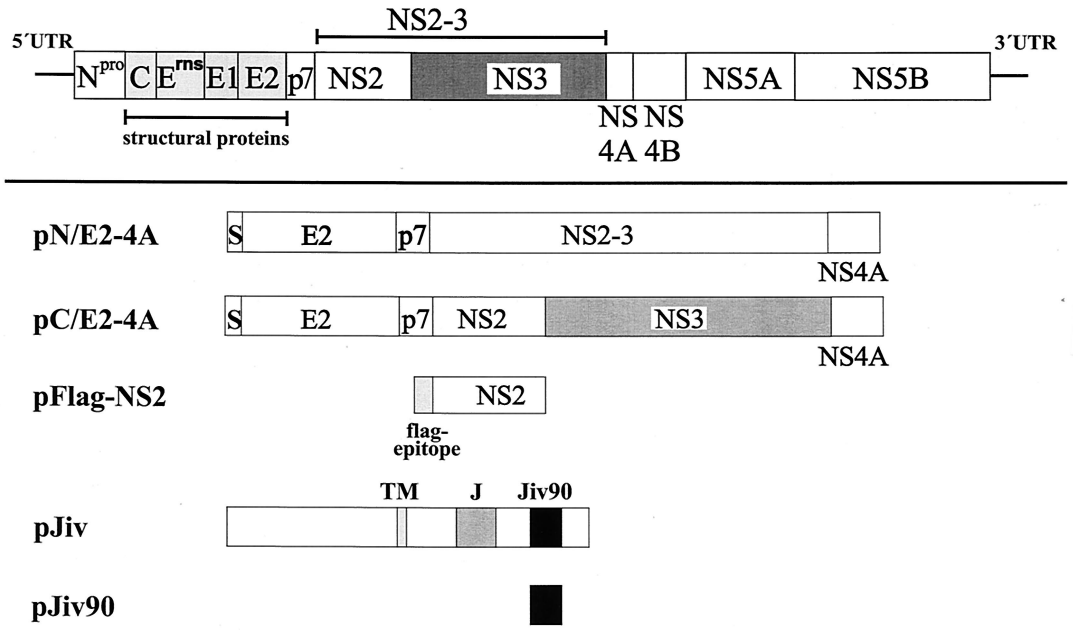

FIG. 3. Scheme of expression constructs. In the upper part of the figure, the BVDV polyprotein is symbolized by a bar; the lines at both ends represent the UTRs. In the lower part of the figure, expression constructs are shown. The box marked with S represents the signal sequence for translocation of E2 into the ER. TM, putative transmembrane domain; J, J domain; Jiv90, Jiv90 domain.

Flag-NS2 (40 kDa) (Fig. 5, lanes 4) or GST-Jiv (110 kDa) (Fig. 5, lanes 7) isolated from cells merely transfected with the corresponding plasmids. According to this experiment, a stable interaction existed between Flag-NS2 and GST-Jiv. In line with these results, the Flag-tag-specific MAb and the anti-GST MAb precipitated Flag-NS2 and a 35-kDa protein (Fig. 5, lanes 9 and 10) from cells cotransfected with pFlag-NS2 and pGST-Jiv90; the 35-kDa protein comigrated with GST-Jiv90 precipitated from cells transfected only with pGST-Jiv90 (Fig. 5, lane 11). As a control, cells cotransfected with pFlag-NS2 and pGST (encoding merely GST) were analyzed by immunoprecipitation with the anti-GST and anti-Flag MAbs, respectively. Each MAb pulled down its specific antigen, namely, GST (30-kDa protein, Fig. 5, lane 13) and Flag-NS2 (Fig. 5, lane 14), respectively, and coprecipitation was not observed. Other controls verified that there was neither a cross-reaction between the anti-Flag MAb and either the GST-Jiv or the GST-Jiv90 (Fig. 5, lanes 8 and 12) nor a cross-reaction between the anti-GST MAb and Flag-NS2 (Fig. 5, lane 3). Additional experiments also gave no indication of an interaction between GST-Jiv or GST-Jiv90 and NS3 expressed from pNS3 (data not shown). These experiments demonstrate a specific and stable

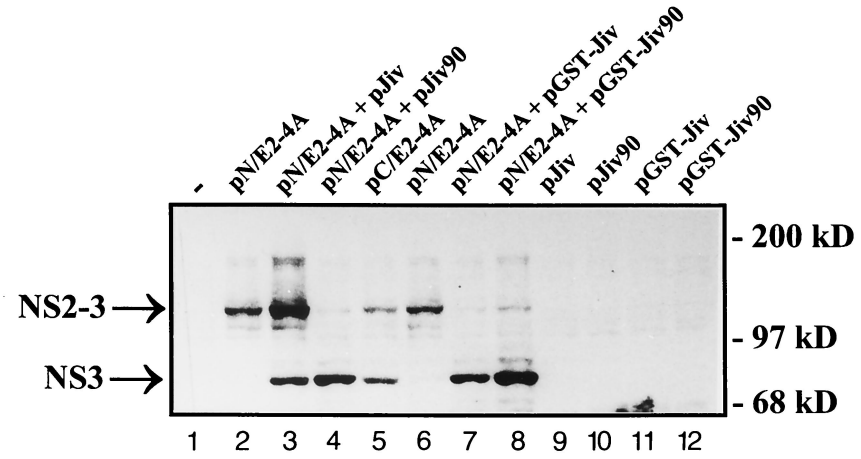

FIG. 4. Western blot analysis. BHK-21 cells infected with MVA-T7pol vaccinia virus were transfected with the plasmids indicated above the lanes. The cell lysates were separated by SDS-PAGE and processed for Western blotting by using an NS3-specific MAb. The positions of NS2-3 and NS3 are indicated on the left. The molecular mass standard is indicated at the right.

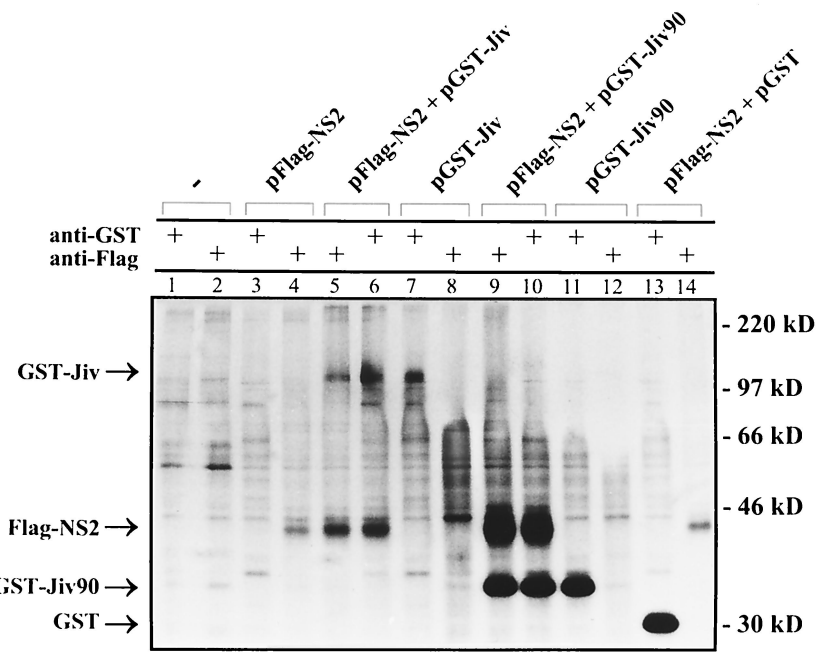

FIG. 5. Coprecipitation analysis. BHK-21 cells infected with MVA-T7pol vaccinia virus were transfected with the plasmids indicated above the respective lanes. Proteins were metabolically labeled and subjected to immunoprecipitation under nondenaturing conditions. The MAbs used for precipitation are indicated. The precipitates were separated by SDS-PAGE and processed for fluorography. Arrowheads on the left mark the positions of GST-Jiv, Flag-NS2, GST-Jiv90, and GST. On the right, the molecular mass standards are indicated.

interaction between Flag-NS2 and Jiv, as well as between Flag-NS2 and Jiv90.

Regulated expression of Jiv. Although Jiv binds to viral NS2 and induces processing of NS2-3, the latter protein is not cleaved to a detectable extent in MDBK cells infected with noncp BVDV. The failure to induce cleavage could be due to a low endogenous level of Jiv in the respective cells. To address this point directly, we used the Tet-On system (8) to establish MDBK cell lines that allow regulated expression of an additional amount of Jiv. The Jiv-ORF was inserted into the Tet-On expression plasmid pTRE; the resulting construct pTRE/Jiv was cotransfected together with a plasmid conferring puromycin resistance into a previously established MDBK cell line ($MDBK_{Tet\text{-}On}$), which constitutively expresses the rtTA activator protein of the Tet-On system. The resulting cell clones were screened for inducible expression of Jiv by immunofluorescence analysis with the anti-Jiv serum (Fig. 6A). Confocal laser-scanning microscopy revealed that recombinant Jiv localizes in membranous structures surrounding the nucleus. According to these results, we assume that Jiv localizes at the endoplasmic reticulum (ER) membrane or in the lumen of the ER.

Radioimmunoprecipitation showed that Jiv isolated from $MDBK_{Tet\text{-}On}$/Jiv cells and Jiv expressed from pJiv by transient vaccinia virus expression experiments exhibited an identical size (Fig. 6B). In the $MDBK_{Tet\text{-}On}$/Jiv cell line, the induction of Jiv expression by various concentrations of the inductor Dox was tested at 45 h postinduction by Western blot using the anti-Jiv serum (Fig. 6C). According to this assay, the intracellular amount of Jiv significantly increased with the concentration of inductor at between 10 nM and 1 μM Dox. Higher Dox concentrations, e.g., 10 μM, did not lead to a significant further increase in the amount of Jiv. No toxic effect of Dox or the Dox-induced Jiv expression was observed.

The obtained $MDBK_{Tet\text{-}On}$/Jiv cell line allows a strictly regulated expression of Jiv. Moreover, Jiv was not detected by Western blotting in naive MDBK cells, thus confirming the assumption that the absence of NS2-3 cleavage observed upon noncp BVDV infection is due to the low amount of Jiv in these cells.

Level of Jiv determines the degree of NS2-3 cleavage. Using the inducible system described above, we tested whether a correlation exists between the intracellular Jiv concentration and the degree of NS2-3 cleavage. $MDBK_{Tet\text{-}On}$/Jiv cells cultured and induced in parallel to the ones used for the analysis shown in Fig. 6C were infected with noncp BVDV strain NCP7 at 18 h postinduction. An analysis of the infected cells was performed by SDS-PAGE and Western blot at 27 h postinfection. At this time point the amount of Jiv in the infected cells correlated directly with the concentration of the inductor (Fig. 7A). In cells grown in the presence of 1 or 10 nM Dox in addition to NS2-3, a faint band of NS3 appeared (Fig. 7B, lanes 4 and 5). When the Dox concentration was increased to 100 nM Dox or more, NS2-3 was efficiently cleaved, as indicated by a high amount of NS3 and a concomitant decrease in the level of NS2-3 (Fig. 7B, lanes 6 to 8). In noninduced cells, the anti-NS3 MAb detected unprocessed NS2-3, whereas no NS3 was found (Fig. 7B, lane 3). These experiments demonstrate the existence of a direct correlation between the intracellular concentration of Jiv and the degree of NS2-3 cleavage in noncp BVDV-infected MDBK cells.

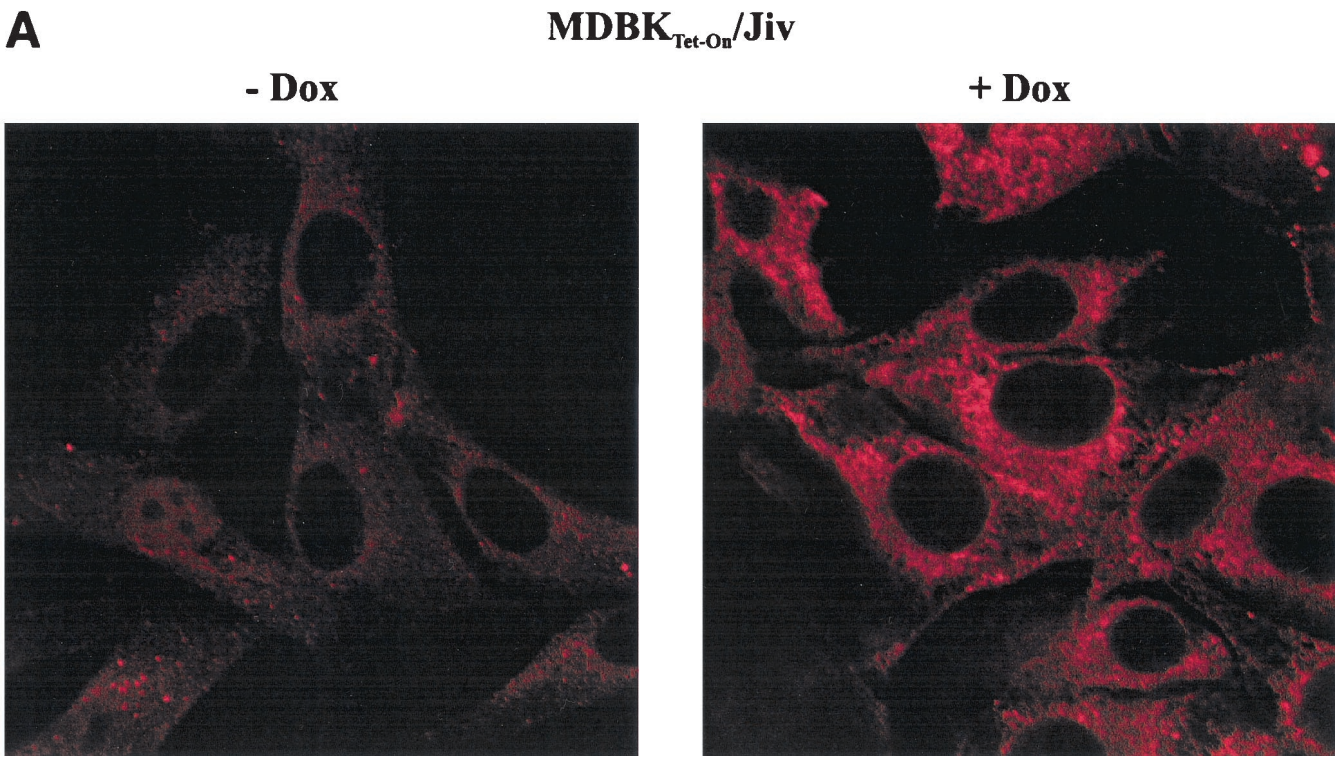

FIG. 6. (A) Immunofluorescence analysis of MDBK$_{Tet-On}$/Jiv cells. Cells cultured in the absence (left) or presence of 10 μM Dox for 24 h (right) were assayed for Jiv expression by the Jiv-specific antiserum and a secondary Cy3-labeled antiserum. The cells were visualized by confocal laser-scanning microscopy. Magnification, ×100. (B) RIPA. BHK-21 cells (two lanes at left) were infected with MVA-T7pol vaccinia virus and transfected with the plasmids indicated above each lane. MDBK or MDBK$_{Tet-On}$/Jiv cells were cultured in the presence of 10 μM Dox for 18 h. Subsequently, the cells were metabolically labeled with [^{35}S]methionine and [^{35}S]cysteine for 6 h. Lysates were prepared from the respective cells under nondenaturing conditions. To minimize background signals, the lysates were subjected to immunoprecipitation with preimmune serum; the supernatants were subsequently used for immunoprecipitation with the Jiv-specific antiserum. The precipitates were analyzed by SDS-PAGE and processed for fluorography. The position of Jiv is indicated. The molecular mass standard is given on the right. (C) Western blot analysis. MDBK and MDBK$_{Tet-On}$/Jiv cells were cultured for 45 h in the presence of the Dox concentrations indicated above the lanes. Lysates of these cells were separated by SDS-PAGE and processed for Western blotting with the Jiv-specific antiserum. The position of Jiv is marked on the right. Molecular mass standards are given on the left.

Switch of viral phenotype. The expression of NS3 represents a hallmark of cp BVDV strains. Since Jiv triggered NS2-3 cleavage, we speculated that the intracellular concentration of Jiv also influences the phenotype of BVDV. To investigate this aspect directly, we infected MDBK$_{Tet-On}$/Jiv cells at 18 h postinduction (10 μM Dox) with noncp BVDV strain NCP7. MDBK$_{Tet-On}$/Jiv cells grown in the absence of inductor as well as naive MDBK cells cultured in presence or absence of Dox, respectively, were also infected with noncp BVDV NCP7 and served as controls. The infection was verified after 24 h by immunofluorescence analysis with the anti-NS3 MAb (data not shown).

Interestingly, the Dox-induced MDBK$_{Tet-On}$/Jiv cell cultures developed a CPE after infection with noncp BVDV NCP7 (Fig. 8). At the time point at which the Dox-induced and NCP7-infected MDBK$_{Tet-On}$/Jiv cell cultures developed a CPE, a significant amount of NS3 was detected (data not shown; see also Fig. 7B). Viruses harvested from the supernatants of these cells exhibited a noncp phenotype when used for infection of normal MDBK cells, and in these cells no cleavage of NS2-3 was detectable (data not shown). Accordingly, the elevation of the intracellular level of Jiv caused the switch of the viral phenotype in the absence of relevant genotypic changes of progeny virus. In contrast, neither MDBK$_{Tet-On}$/Jiv cells grown in the absence of inductor nor any of the other cell cultures that served as controls showed a CPE after infection with NCP7 (Fig. 8). Corresponding results were obtained, e.g., for noncp BVDV strain NCP1 (21) (data not shown), verifying that the observed effect is not restricted to strain NCP7. In a control experiment, rabies virus displayed a noncp phenotype in noninduced as well as in induced MDBK$_{Tet-On}$/Jiv cells (data not shown). In summary, these data demonstrate that the intracellular level of Jiv determines specifically the phenotype of BVDV.

DISCUSSION

Positive-strand RNA viruses encode polyproteins, which are cleaved by virus-encoded and often also by cellular proteases to generate the mature viral proteins. Fidelity and regulation of the kinetics of polyprotein processing are crucial for bona fide replication of these viruses. Mutations leading to deregulation of the activity of an alphaviral protease can be correlated with a reduced replication level and result in a loss of viral

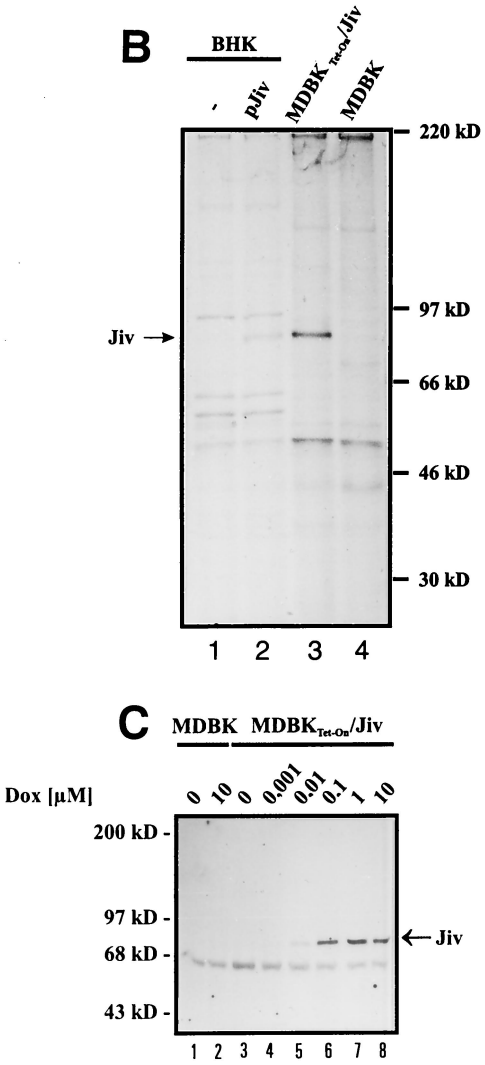

FIG. 6.—*Continued.*

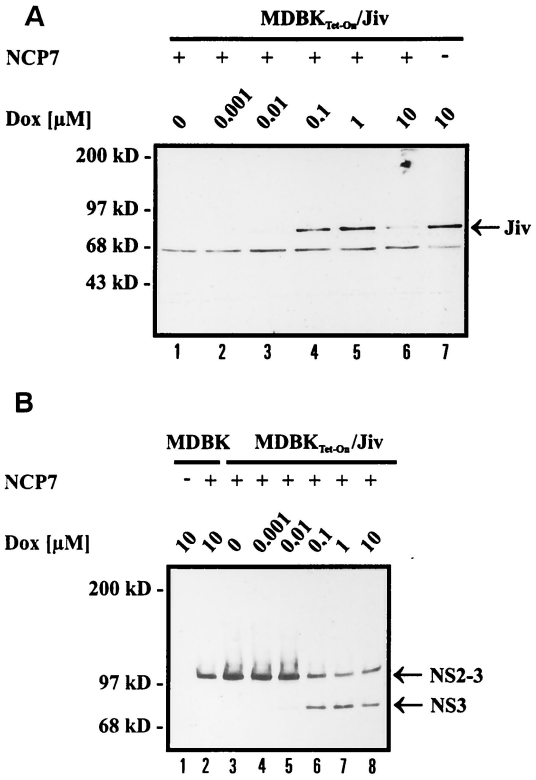

FIG. 7. Western blot analysis. (A) $MDBK_{Tet\text{-}On}$/Jiv cells were infected with noncp BVDV strain NCP7 at an MOI of 0.01 at 18 h postinduction (the concentrations of Dox are indicated above the lanes). Cell lysates were prepared 27 h postinfection, separated by SDS-PAGE, and processed for Western blot with Jiv-specific antiserum. The position of Jiv is marked on the right. Molecular mass standards are indicated. Compared to noninfected cells, the NCP7-infected $MDBK_{Tet\text{-}On}$/Jiv cells contained, upon induction by 10 μM Dox, a smaller amount of Jiv (lane 6); a possible explanation for this observation is a degradation of Jiv with the onset of apoptosis in the infected cells. (B) MDBK and $MDBK_{Tet\text{-}On}$/Jiv cells were treated as described in panel A. After SDS-PAGE, the anti-NS3 MAb was applied for Western blot analysis. Arrowheads on the right mark the positions of NS2-3 and NS3.

cytopathogenicity (7). In the case of the pestivirus BVDV, the viral phenotype strictly correlates with one specific processing event in the viral polyprotein, namely, an efficient release of NS3 from the polyprotein, which has been shown to be essential for the cytopathogenicity of BVDV (17, 20, 39). For cp BVDV, diverse genomic alterations have been described, all leading to the generation of NS3 (reviewed in reference 23). Thus far, all of these mutations directly concerned the genomic region coding for NS2-3 of cp BVDV. In the present study, we demonstrate for the first time that NS2-3 from noncp BVDV can also be efficiently processed when stimulated by a cellular protein in *trans*. The trigger for this processing event is an increased intracellular level of an as-yet-uncharacterized cellular protein of the J-domain family. All members of this highly heterogeneous family of chaperones encompass the J domain as the only common characteristic (reviewed in references 2 and 12). One of the best-studied J-domain proteins is the *E. coli* protein DnaJ (eukaryotic homolog, Hsp40). In DnaJ the N-terminal J domain is followed by a glycine-phenylalanine (G/F) region and a cysteine-rich domain composed of four CXXCXGXG motifs, which coordinate two Zn^{2+} ions (15, 38). DnaJ has been shown to interact with hydrophobic regions of partially folded proteins via its cysteine-rich domain and to mediate their transfer to DnaK, a chaperone of the Hsp70 family (38). Members of the latter protein family function mainly in preventing the aggregation of newly synthesized, unfolded proteins. The J domain mediates binding of DnaJ to DnaK. DnaJ triggers the ATPase activity of DnaK and thereby the transfer of the partially folded peptide to the cellular folding machinery (48). In eukaryotes, additional J-domain proteins with highly specialized functions have been described. Auxilin, for example, forms part of the clathrin baskets of clathrin coated vesicles (46). The constitutively expressed mammalian Hsp70 family member Hsc73 has been shown to catalyze the disassembly of the clathrin coats. Auxilin assists in the positioning of Hsc73 and the disassembly process. The J-domain yeast protein Sec63p is a component of the protein translocation machinery at the ER (53). Mammalian Sec63p resides at the ER membrane and is believed to be involved in

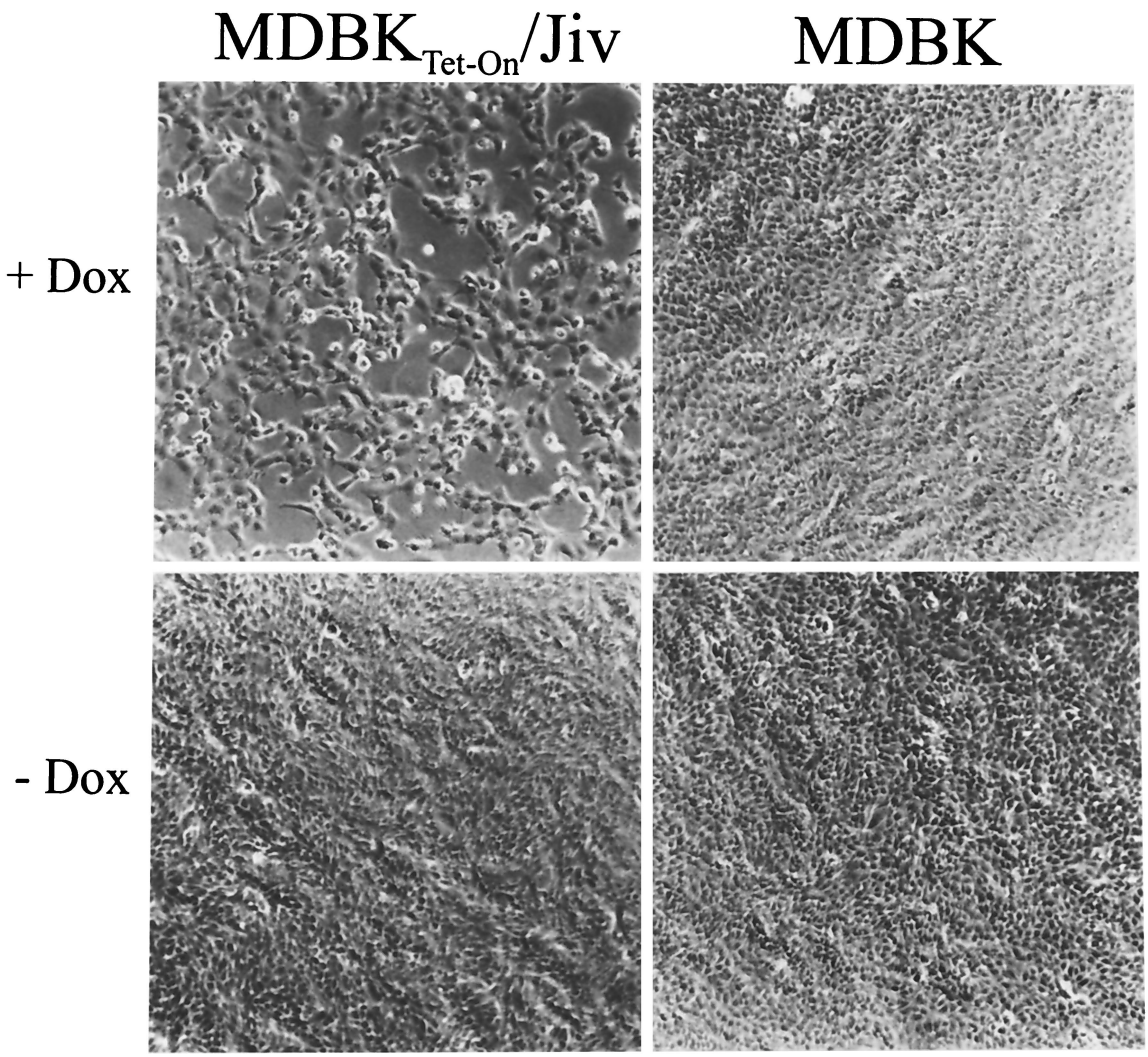

FIG. 8. Cell morphology. MDBK and MDBK$_{Tet-On}$/Jiv cells were cultured in the absence or presence of 10 μM Dox. At 18 h postinduction, the cells were infected with noncp BVDV strain NCP7 at an MOI of 0.5. Cells were fixed at 24 h postinfection and visualized by phase-contrast microscopy. Magnification, ×100.

membrane integration and/or the translocation of proteins. For human Sec63p, an interaction with a Hsp70 residing in the lumen of the ER was demonstrated (45). A role for J-domain proteins has also been implicated, e.g., in exocytosis, mitochondrial protein import, and cell cycle regulation (2, 12). Taken together, these findings indicate that J-domain proteins are chaperones with important regulatory functions in protein folding processes in prokaryotes as well as in eukaryotes. They target the members of the Hsp70 family to their substrates. For their coordinative function, the J-domain proteins possess different domains, each specialized for protein-protein interaction.

The J-domain protein characterized in this study, Jiv, shares only in the J domain a significant degree of homology with DnaJ. In this respect, Jiv resembles a large group of J-domain proteins, including auxilin and Sec63p. We suggest for Jiv, similar to Sec63p, a localization at the ER; this hypothesis is based mainly on our microscopy data (Fig. 6A). In line with these observations, a computer-assisted PSORT analysis (25) predicted a localization of Jiv at the ER membrane (data not shown). In preliminary experiments, Jiv displayed a similar localization to that of heme oxygenase-1, a marker molecule of the ER membrane (data not shown). The J domain of Jiv resides in the central region of the molecule, which represents another analogy to Sec63p. Since J domains in general mediate the interaction with specific Hsp70s, it seems likely that Jiv recruits a specific member of the Hsp70 family via its J domain. Moreover, this study substantiates the presence of another protein-binding domain in Jiv; this domain with a length of not more than 90 amino acids (Jiv90) specifically binds to NS2 of BVDV. Orthologs of Jiv, which also encompass a J domain followed by a Jiv90 homolog domain, were identified in several species, ranging from the nematode *C. elegans* to *Homo sapiens* (Fig. 2); however, despite Jiv's high conservation throughout phylogeny, we were not able to identify a Jiv ortholog in yeast or *E. coli*. It is tempting to speculate that the Jiv90 domain also mediates binding to one or more cellular interaction partners. The identification of these ligands could provide insight into

the biological function of Jiv within the cell. Because of its localization presumably at or in the ER (Fig. 6B), a role for Jiv in protein folding processes associated with membrane insertion and/or the translocation of proteins is conceivable. Other characteristics of Jiv that can be deduced from its primary sequence include one putative transmembrane domain and two CXXCXXXH motifs. These motifs are located in the Jiv90 domain and might in analogy to the cysteine-rich domain of DnaJ (CXXCXGXG motif) represent a structurally important Zn-binding domain with the capacity to coordinate one Zn^{2+} ion. Since the Zn-binding domain of DnaJ was shown to be involved in the interaction with denatured protein substrates (38), it is likely that the corresponding motif in Jiv90 might contribute to NS2 binding.

For Jiv/Jiv90 different roles in the cleavage of NS2-3 are conceivable, namely, a proteolytic activity or the induction of a conformational change in NS2-3, leading to processing by a viral or cellular protease. Our data do not support a proteolytic activity of Jiv or Jiv90 for the following reasons. (i) To our knowledge, Jiv90 would represent the shortest protease active in *trans* characterized thus far. (ii) We could not identify any motif characteristic for proteases in the primary sequence of Jiv90. (iii) We observed that the extent of NS2-3 cleavage in BVDV-infected cells is strictly correlated to the intracellular level of Jiv (Fig. 7B). (iv) Western blot analyses indicate that similar amounts of both proteins are necessary to achieve an optimal cleavage efficiency (Fig. 7B and data not shown). (v) The stable interaction of Jiv with NS2 also argues against a proteolytic function of Jiv.

Instead, it appears likely that the observed binding of Jiv or Jiv90 leads to a conformational change of NS2-3. The N-terminal region of NS2 has a hydrophobic character and, upon expression in the vaccinia virus system, the NS2 protein can be detected in the same perinuclear compartment as Jiv (data not shown). It is therefore possible that Jiv modulates the membrane topology of NS2-3. A change in the conformation of NS2-3 could expose the cleavage site and allow proteolytic processing by a protease. On the basis of the discussion presented above, we suggest an intrinsic protease located within NS2-3; according to this model, the intrinsic protease would be activated by the Jiv-induced conformational change. For the NS2 of some cp BVDV strains, a protease activity catalyzing the cleavage of NS2-3 has been proposed (14, 41). Preliminary data obtained by a mutagenesis study are also in line with the existence of a protease domain in NS2 (data not shown). In this context, it is particularly noteworthy that NS2-3 cleavage of the closely related HCV is catalyzed by a viral protease residing in NS2-3 (11, 28, 31). It remains to be clarified whether Jiv also plays a role in the fine-tuning of NS2-3 cleavage in the HCV system. On the basis of in vitro studies, the involvement of the cellular chaperone system in the proper folding of NS2 has already been suggested (26).

The ability to establish a lifelong persistent infection after diaplacental exposure is crucial for the maintenance of BVDV in the field (43). This feature is strictly limited to the noncp phenotype of BVDV. Thus, controlling the activity of the putative NS2 protease in the noncp BVDV polyprotein by limiting the amounts of the cellular cofactor Jiv might represent an important regulatory mechanism for the virus. It will be particularly interesting to determine whether the interaction between Jiv and NS2 is even essential for the replication of BVDV. It is obvious that Jiv represents an excellent subject to study virus-host cell interaction and its involvement in viral replication and cytopathogenicity. Moreover, the knowledge of a natural binding partner of the J-domain protein Jiv should significantly facilitate the elucidation of its cellular function.

ACKNOWLEDGMENTS

We thank S. Jakobi for excellent technical assistance and M. König for support in the rabies virus control experiment. We are grateful to J. Baumeister and R. Schneider for contributions in the initial phase of the project.

This study was supported by the SFB 535 "Invasionsmechanismen und Replikationsstrategien von Krankheitserregern" from the Deutsche Forschungsgemeinschaft.

REFERENCES

1. **Becher, P., G. Meyers, A. D. Shannon, and H. J. Thiel.** 1996. Cytopathogenicity of border disease virus is correlated with integration of cellular sequences into the viral genome. J. Virol. **70:**2992–2998.
2. **Cheetham, M. E., and A. J. Caplan.** 1998. Structure, function and evolution of DnaJ: conservation and adaptation of chaperone function. Cell Stress Chaperones **3:**28–36.
3. **Collett, M. S., R. Larson, C. Gold, D. Strick, D. K. Anderson, and A. F. Purchio.** 1988. Molecular cloning and nucleotide sequence of the pestivirus bovine viral diarrhea virus. Virology **165:**191–199.
4. **Corapi, W. V., R. O. Donis, and E. J. Dubovi.** 1990. Characterization of a panel of monoclonal antibodies and their use in the study of the antigenic diversity of bovine viral diarrhea virus. Am. J. Vet. Res. **51:**1388–1394.
5. **Corapi, W. V., R. O. Donis, and E. J. Dubovi.** 1988. Monoclonal antibody analyses of cytopathic and noncytopathic viruses from fatal bovine viral diarrhea infections. J. Virol. **62:**2823–2827.
6. **Devereux, J., P. Haeberli, and O. A. Smithies.** 1984. A comprehensive set of sequence analysis programs for the VAX. Nucleic Acids Res. **12:**387–395.
7. **Frolov, I., E. Agapov, T. A. Hoffman, Jr., B. M. Pragai, M. Lippa, S. Schlesinger, and C. M. Rice.** 1999. Selection of RNA replicons capable of persistent noncytopathic replication in mammalian cells. J. Virol. **73:**3854–3865.
8. **Gossen, M., S. Freundlieb, G. Bender, G. Muller, W. Hillen, and H. Bujard.** 1995. Transcriptional activation by tetracyclines in mammalian cells. Science **268:**1766–1769.
9. **Harada, T., D. W. Kim, K. Sagawa, T. Suzuki, K. Takahashi, I. Saito, Y. Matsuura, and T. Miyamura.** 1995. Characterization of an established human hepatoma cell line constitutively expressing non-structural proteins of hepatitis C virus by transfection of viral cDNA. J. Gen. Virol. **76:**1215–1221.
10. **Harada, T., N. Tautz, and H.-J. Thiel.** 2000. E2-p7 region of the bovine viral diarrhea virus polyprotein: processing and functional studies. J. Virol. **74:**9498–9506.

10a. **Harlow, E., and D. Lane.** 1988. Antibodies: a laboratory manual. Cold Spring Harbor Laboratory Press, Cold Spring Harbor, N.Y.

11. **Hijikata, M., H. Mizushima, T. Akagi, S. Mori, N. Kakiuchi, N. Kato, T. Tanaka, K. Kimura, and K. Shimotohno.** 1993. Two distinct proteinase activities required for the processing of a putative nonstructural precursor protein of hepatitis C virus. J. Virol. **67:**4665–4675.
12. **Kelley, W. L.** 1998. The J-domain family and the recruitment of chaperone power. Trends Biochem. Sci. **23:**222–227.
13. **Kozak, M.** 1986. Point mutations define a sequence flanking the AUG initiator codon that modulates translation by eukaryotic ribosomes. Cell **44:**283–292.
14. **Kümmerer, B. M., and G. Meyers.** 2000. Correlation between point mutations in NS2 and the viability and cytopathogenicity of bovine viral diarrhea virus strain Oregon analyzed with an infectious cDNA clone. J. Virol. **74:**390–400.
15. **Martinez-Yamout, M., G. B. Legge, O. Zhang, P. E. Wright, and H. J. Dyson.** 2000. Solution structure of the cystein-rich domain of the *Escherichia coli* chaperone protein DnaJ. J. Mol. Biol. **300:**805–818.
16. **McClurkin, A. W., M. F. Coria, and S. R. Bolin.** 1985. Isolation of cytopathic and noncytopathic bovine viral diarrhea virus from the spleen of cattle acutely and chronically affected with bovine viral diarrhea. J. Am. Vet. Med. Assoc. **186:**568–569.
17. **Mendez, E., N. Ruggli, M. S. Collett, and C. M. Rice.** 1998. Infectious bovine viral diarrhea virus (strain NADL) RNA from stable cDNA clones: a cellular insert determines NS3 production and viral cytopathogenicity. J. Virol. **72:**4737–4745.
18. **Meyers, G., T. Rümenapf, and H.-J. Thiel.** 1990. Insertion of ubiquitin-coding sequence identified in the RNA genome of a togavirus, p. 25–29. *In* M. A. Brinton and F. X. Heinz (ed.), New aspects of positive-strand RNA

viruses. American Society for Microbiology, Washington, D.C.
19. **Meyers, G., T. Rümenapf, and H.-J. Thiel.** 1989. Ubiquitin in a togavirus. Nature **341:**491.
20. **Meyers, G., N. Tautz, P. Becher, H.-J. Thiel, and B. Kümmerer.** 1996. Recovery of cytopathogenic andnoncp bovine viral diarrhea viruses from cDNA constructs. J. Virol. **70:**8606–8613.
21. **Meyers, G., N. Tautz, E. J. Dubovi, and H.-J. Thiel.** 1991. Viral cytopathogenicity correlated with integration of ubiquitin-coding sequences. Virology **180:**602–616.
22. **Meyers, G., N. Tautz, R. Stark, J. Brownlie, E. J. Dubovi, M. S. Collett, and H.-J. Thiel.** 1992. Rearrangement of viral sequences in cytopathogenic pestiviruses. Virology **191:**368–386.
23. **Meyers, G., and H.-J. Thiel.** 1996. Molecular characterization of pestiviruses. Adv. Virus Res. **47:**53–118.
24. **Mizushima, S., and S. Nagata.** 1990. pEF-BOS, a powerful mammalian expression vector. Nucleic Acids Res. **18:**5322.
25. **Nakai, K., and M. Kanehisa.** 1992. A knowledge base for predicting protein localization sites in eukaryotic cells. Genomics **14:**897–911.
26. **Pieroni, L., E. Santolini, C. Fipaldini, L. Pacini, G. Migliaccio, and N. La Monica.** 1997. In vitro study of the NS2-3 protease of hepatitis C virus. J. Virol. **71:**6373–6380.
27. **Reed, K. E., A. E. Gorbalenya, and C. M. Rice.** 1998. The NS5A/NS5 proteins of viruses from three genera of the family *Flaviviridae* are phosphorylated by associated serine/threonine kinases. J. Virol. **72:**6199–6206.
28. **Reed, K. E., A. Grakoui, and C. M. Rice.** 1995. Hepatitis C virus-encoded NS2-3 protease: cleavage-site mutagenesis and requirements for bimolecular cleavage. J. Virol. **69:**4127–4136.
29. **Renard, A., D. Dino, and J. Martial.** January 1987. Vaccines and diagnostics derived from bovine diarrhea virus. European patent 02.08672.
30. **Ridpath, J. F., and J. D. Neill.** 2000. Detection and characterization of genetic recombination in cytopathic type 2 bovine viral diarrhea viruses. J. Virol. **74:**8771–8774.
31. **Santolini, E., L. Pacini, C. Fipaldini, G. Migliaccio, and N. La Monica.** 1995. The NS2 protein of hepatitis C virus is a transmembrane polypeptide. J. Virol. **69:**7461–7471.
32. **Schägger, H., and G. von Jagow.** 1987. Tricine-sodium dodecyl sulfate-polyacrylamide gel electrophoresis for the separation of proteins in the range from 1 to 100 kDa. Anal. Biochem. **166:**368–379.
33. **Schneider, R., G. Unger, R. Stark, E. Schneider-Scherzer, and H.-J. Thiel.** 1993. Identification of a structural glycoprotein of an RNA virus as a ribonuclease. Science **261:**1169–1171.
34. **Schultz, J., R. R. Copley, T. Doerks, C. P. Ponting, and P. Bork.** 2000. SMART: a web-based tool for the study of genetically mobile domains. Nucleic Acids Res. **28:**231–234.
35. **Stark, R., G. Meyers, T. Rümenapf, and H.-J. Thiel.** 1993. Processing of pestivirus polyprotein: cleavage site between autoprotease and nucleocapsid protein of classical swine fever virus. J. Virol. **67:**7088–7095.
36. **Steffens, S., H.-J. Thiel, and S.-E. Behrens.** 1999. The RNA-dependent RNA polymerases of different members of the family *Flaviviridae* exhibit similar properties in vitro. J. Gen. Virol. **80:**2583–2590.
37. **Sutter, G., M. Ohlmann, and V. Erfle.** 1995. Non-replicating vaccinia vector efficiently expresses bacteriophage T7 RNA polymerase. FEBS Lett. **371:**9–12.
38. **Szabo, A., R. Korszun, F. U. Hartl, and J. Flanagan.** 1996. A zinc finger-like domain of the molecular chaperone DnaJ is involved in binding to denatured protein substrates. EMBO J. **15:**408–417.
39. **Tautz, N., T. Harada, A. Kaiser, G. Rinck, S. E. Behrens, and H.-J. Thiel.** 1999. Establishment and characterization of cytopathogenic and noncytopathogenic pestivirus replicons. J. Virol. **73:**9422–9432.
40. **Tautz, N., A. Kaiser, and H. J. Thiel.** 2000. NS3 serine protease of bovine viral diarrhea virus: characterization of active site residues, NS4A cofactor domain, and protease-cofactor interactions. Virology **273:**351–363.
41. **Tautz, N., G. Meyers, R. Stark, E. J. Dubovi, and H.-J. Thiel.** 1996. Cytopathogenicity of a pestivirus correlated with a 27-nucleotide insertion. J. Virol. **70:**7851–7858.
42. **Tautz, N., G. Meyers, and H.-J. Thiel.** 1993. Processing of poly-ubiquitin in the polyprotein of an RNA virus. Virology **197:**74–85.
43. **Thiel, H.-J., P. G. W. Plagemann, and V. Moennig.** 1996. Pestiviruses, p. 1059–1073. *In* B. N. Fields, D. M. Knipe, and P. M. Howley (ed.), Fields virology, 3rd ed., vol. 1. Lippincott-Raven Publishers, Philadelphia, Pa.
44. **Thiel, H.-J., R. Stark, E. Weiland, T. Rümenapf, and G. Meyers.** 1991. Hog cholera virus: molecular composition of virions from a pestivirus. J. Virol. **65:**4705–4712.
45. **Tyedmers, J., M. Lerner, C. Bies, J. Dudek, M. H. Skowronek, I. G. Haas, N. Heim, W. Nastainczyk, J. Volkmer, and R. Zimmermann.** 2000. Homologs of the yeast Sec complex subunits Sec62p and Sec63p are abundant proteins in dog pancreas microsomes. Proc. Natl. Acad. Sci. USA **97:**7214–7219.
46. **Ungewickell, E., H. Ungewickell, and S. E. Holstein.** 1995. Role of auxilin in the uncoating clathrin-coated vesicles. Nature **378:**632–635.
47. **Vilcek, S., I. Greiser-Wilke, P. Nettleton, and D. J. Paton.** 2000. Cellular insertions in the NS2-3 genome region of cytopathic bovine viral diarrhoea virus (BVDV) isolates. Vet. Microbiol. **77:**129–136.
48. **Wall, D., M. Zylicz, and C. Georgopoulos.** 1994. The NH2-terminal 108 amino acids of the *Escherichia coli* DnaJ protein stimulate the ATPase activity of DnaK and are sufficient for lambda replication. J. Biol. Chem. **269:**5446–5451.
49. **Wiskerchen, M., S. K. Belzer, and M. S. Collett.** 1991. Pestivirus gene expression: the first protein product of the bovine viral diarrhea virus large open reading frame, P20, possesses proteolytic activity. J. Virol. **65:**4508–4514.
50. **Wiskerchen, M., and M. S. Collett.** 1991. Pestivirus gene expression: protein p80 of bovine viral diarrhea virus is a proteinase involved in polyprotein processing. Virology **184:**341–350.
51. **Xu, J., E. Mendez, P. R. Caron, C. Lin, M. A. Murcko, M. S. Collett, and C. M. Rice.** 1997. Bovine viral diarrhea virus NS3 serine proteinase: polyprotein cleavage sites, cofactor requirements, and molecular model of an enzyme essential for pestivirus replication. J. Virol. **71:**5312–5322.
52. **Zhong, W., L. L. Gutshall, and A. M. Del Vecchio.** 1998. Identification and characterization of an RNA-dependent RNA polymerase activity within the nonstructural protein 5B region of bovine viral diarrhea virus. J. Virol. **72:**9365–9369.
53. **Zimmermann, R.** 1998. The role of molecular chaperones in protein transport into the mammalian endoplasmatic reticulum. Biol. Chem. **379:**275–282.